Analysis of the Remarkable Difference in the Stabilities of Methyl- and Ethyldiazonium Ions

Rainer Glaser,* Godwin Sik-Cheung Choy, and M. Kirk Hall

Contribution from the Department of Chemistry, University of Missouri—Columbia, Columbia, Missouri 65211. *Received August 22, 1990*

Abstract: A remarkable difference of 30.7 kcal/mol has been determined for the dediazoniation enthalpies of methyldiazonium ion (**1**) (ΔH = 42.2 kcal/mol) and ethyldiazonium ion (**2**) (ΔH = 11.5 kcal/mol) at a theoretical level that is shown to well reproduce the experimental methyl cation affinity of N_2. Only a small part (5.6 kcal/mol) of this stability difference may be accounted for by the production of the nonclassical ethyl cation in the dissociation of **2**. The intrinsic differences in the CN linkages in **1** and **2** are analyzed in a variety of ways. Electron density analysis at correlated levels confirms that diazonium ions are best described as carbocations and that they are inadequately described by the commonly accepted Lewis notations; the overall electron transfer from N_2 to the carbocation on formation of the diazonium ions is small. A new method is described for the evaluation of electrostatic contributions to bonding based on atom-centered charges and atomic dipole moments. This method together with an analysis of the binding energies in terms of fragment stabilities reveals the two major reasons for the large difference in the binding energies: the reduction of the electrostatic contribution to CN binding in **2** compared to **1** and the comparatively larger destabilization of the diazo group in **2** with regard to free N_2. CN bonding in both diazonium ions results because of stabilization of the hydrocarbon fragment and despite the destabilization of the diazo group. The structural and topological features of the CN linkages in **1** and **2** are similar, and their consideration alone cannot account for the large difference in their dissociation energies. These results emphasize that, in general, the characterization of the electron density in the bonding region alone is not sufficient to fully characterize all of the bond properties.

Introduction

Alkyldiazonium ions are highly reactive intermediates in a variety of important deamination reactions,[1] and they usually are considered as the reactive species responsible for the mutagenic modification of cellular constituents and, specifically, for the alkylation of DNA.[2-7] The transient character of alkyldiazonium ions has made it rather difficult to characterize these important intermediates by physical organic techniques.[8] Accurate information about the potential energy surfaces and the electronic structures of the alkyldiazonium ions is scarce, although such knowledge represents one of the essential prerequisites for a more complete understanding of their chemistry. For example, experimental studies have shown that methyl- and ethyldiazonium ions exhibit a distinct difference in their site preference in the alkylation of DNA. While methylation occurs preferentially at the N centers, ethylation differentiates significantly less between the O and the N nucleophiles.

In this paper, we report on the results of a comparative ab initio study of methyldiazonium ion (**1**) and ethyldiazonium ion (**2**). The potential energy surfaces of **1** and **2** have been explored both at the restricted Hartree–Fock level and with the inclusion of perturbational corrections for electron correlation, and the thermodynamic stabilities with regard to dediazoniation (eq 1) and automerization (eq 2) have been determined. The dediazoniation of **1** had been studied experimentally, and this reaction has therefore been investigated at several higher levels of theory to assure the accuracy of the theoretical levels employed here. A remarkably large difference in the stabilities of **1** and **2** toward dediazoniation is found. It is shown that only a small part of this stability difference may be accounted for by the production of the nonclassical cation in the dissociation of **2**. Electron density analysis was employed in several ways to study this large intrinsic difference in the CN linkages in **1** and **2**. We first analyze the effects of electron correlation on the electron density functions and on the associated topological and integrated properties and then discuss consequences for the bonding model that we recently proposed on the basis of the electronic structures of a series of prototypical diazonium ions with C(sp^3), C(sp^2), and C(sp) carbon involvement in the CN linkages.[9] We then describe a new method for the evaluation of electrostatic contributions to the CN binding which is based on atom-centered charges and dipole moments, and we compare this new method to the results of an analysis of the binding energies in terms of fragment stabilizations, a method that we have described recently.[10]

$$(RNN)^+ \rightarrow R^+ + N_2 \quad (1)$$

$$(RN^*N)^+ \rightarrow R(NN^*)^+ \quad (2)$$

Computational Methods

Geometry optimizations were performed under the constraints of the symmetry point groups indicated with the gradient algorithms of either Schlegel or Baker using both Gaussian88[11] and Gamess.[12] The Hessian matrix was then computed analytically (RHF level) or numerically (MP2 level) for each of the structures to confirm that an extremum on the potential energy surface had indeed been located, to characterize the stationary structures as minima, transition-state structures, or second-order saddle points via the number of negative eigenvalues, and to determine the harmonic vibrational frequencies, the IR intensities, and the vibrational zero-point energies (VZPEs). VZPE corrections to relative energies that were determined at the RHF level have been scaled by the usual factor of 0.9 to account for the typical overestimation at this level.[13]

(1) Review: Kirmse, W. *Angew. Chem., Int. Ed. Engl.* **1976**, *415*, 251.
(2) For reviews see: *Chemical Carcinogens*, 2nd ed.; Searle, C. E., Ed.; ACS Monograph 182; American Chemical Society: Washington, DC, 1984; Chapters 12-14.
(3) Smith, R. H.; Koepke, S. R.; Tondeur, Y.; Denlinger, C. L.; Michejda, C. L. *J. Chem. Soc., Chem. Commun.* **1985**, 936.
(4) (a) Sullivan, J. P.; Wong, J. L. *Biochim. Biophys. Acta* **1977**, *479*, 1. (b) Yuspa, S. H.; Poirier, M. C. *Adv. Cancer Res.* **1987**, *450*, 25.
(5) For studies of the reactions of aryldiazonium ions with adenine and guanine, see: (a) Chin, A.; Hung, M.-H.; Stock, L. M. *J. Org. Chem.* **1981**, *46*, 2203. (b) Hung, M.-H.; Stock, L. M. *J. Org. Chem.* **1982**, *47*, 448.
(6) Hopfinger, A. J.; Mohammad, S. N. *J. Theor. Biol.* **1980**, *87*, 401.
(7) (a) Ford, G. P.; Scribner, J. D. *J. Am. Chem. Soc.* **1983**, *105*, 349. (b) Sapse, A.-M.; Allen, E. B.; Lown, J. W. *J. Am. Chem. Soc.* **1988**, *110*, 5671.
(8) Alkyldiazonium ions have been observed in superacid media (see ref 9 for a summary of references), and methyldiazonium ion has been studied in the gas phase (see refs 25 and 27). In the solid state, alkyldiazonium ions can be stabilized in transition element complexes, but the alkyldiazonium ligands greatly differ from the free ions (see ref 9).
(9) Glaser, R. *J. Phys. Chem.* **1989**, *93*, 7993.
(10) Glaser, R. *J. Comput. Chem.* **1990**, *11*, 663.
(11) Gaussian88 (Rev. C): Frisch, M. J.; Head-Gordon, M.; Schlegel, H. B.; Raghavachari, K.; Binkley, J. S.; Gonzales, C.; Defrees, D. J.; Fox, D. J.; Whiteside, R. A.; Seeger, R.; Melius, C. F.; Baker, J.; Martin, R. L.; Kahn, L. R.; Stewart, J. J. P.; Fluder, E. M.; Topiol, S.; Pople, J. A. Gaussian, Inc., Pittsburgh, PA, 1988. A few calculations were carried out at Yale University with Gaussian90 liscensed to Dr. Wiberg. We are indebted to Dr. Wiberg for computer time.
(12) Gamess: Schmidt, W. M.; Boatz, J. A.; Baldridge, K. K.; Koseki, S.; Gordon, M. S.; Elbert, S. T.; Lam, B. *QCPE Bull.* **1987**, *7*, 115.
(13) Hehre, W. J.; Radom, L.; Schleyer, P. v. R.; Pople, J. A. *Ab Initio Molecular Orbital Theory*; Wiley: New York, 1986; p 226ff.

0002-7863/91/1513-1109$02.50/0

Table I. Energies and Vibrational Zero-Point Energies Determined at RHF/6-31G* and MP2(full)/6-31G*[a]

	RHF/6-31G*			MP2(full)/6-31G*					
	$-E$(RHF)	VZPE	CSS	$-E$(MP2)	VZPE	CSS	ΔH	ΔS	ΔG
1a	148.216 056	30.71	M	148.666 119	28.73	M	31.65	58.27	14.27
1b	148.177 470	26.41	TS	148.600 646	25.59	TS	28.46	62.10	9.94
2a	187.264 411	49.71	M	187.848 720	47.26	M	50.26	68.48	29.79
2b	187.258 801	49.58	TS						
2c	187.255 794	44.84	TS	187.824 361	42.94	TS	46.92	75.95	24.28
2d	187.255 690	44.78	SOSP						
Me^+	39.230 640	21.16	M	39.329 435	20.40	M	22.78	44.40	9.54
3a	78.311 232	40.45	M						
3c	78.309 335	40.14	TS						
3c[b]	78.309 943	40.81	M	78.561 449	39.49	M	42.02	54.22	25.86
3d	78.310 209	40.27	TS	78.551 242	38.48	TS	40.99	55.72	24.38
N_2	108.943 950	3.94	M	109.261 574	3.12	M	5.19	45.70	−8.43

[a] Total energies ($-E$) in atomic units. Unscaled vibrational zero-point energies (VZPE) and thermochemical values in kilocalories per mole. CSS = character of stationary structure (M = minimum, TS = transition structure, SOSP = second-order saddle point structure). [b] Calculated in C_s symmetry.

Thermodynamical functions were derived from the molecular partition functions (translation, rotation, vibration) at the MP2(full)/6-31G* level by using the frequencies as calculated. The program Spectrum[14] was written to display the calculated IR spectra in graphical form.

In general, structural optimizations and the normal mode analyses were carried out at the restricted Hartree–Fock (RHF) level and with the inclusion of the perturbational effects of electron correlation at the second-order Møller–Plesset[15] level with the 6-31G* basis set,[16] MP2-(full)/6-31G*. More reliable energies were then computed with the MP2(full)/6-31G* geometries at the full fourth-order level of Møller–Plesset perturbation theory in the frozen core approximation with the basis set 6-31G* and with the valence-triple-zeta basis set 6-311G**. The dissociation of methyldiazonium ion also was studied at the MP2-(full)/6-311G** level, and for this reaction, correlated energies were determined with the larger basis sets 6-311++G**, 6-311G(df,p), and 6-311++G(df,p).[17]

Electron density analyses[18] were carried out at the RHF level and with the inclusion of perturbational corrections for electron correlation at the MP2 level. The correlated densities were calculated with Frisch's implementation of the Z vector method.[19] The RHF wave functions and MP2 density matrices were transformed into a format suitable for the electron density analysis programs with the program Psichk.[20] Topological and integrated properties of the electron density functions were determined with Bader's programs Extreme and Proaim.[21] Cross sections of the electron densities were determined with the program Netz,[22] and programs were written within the PV-Wave programming environment for their display in two- or three-dimensional form. The programs Dipoles[22] and ESI[23] were written to analyze the properties of the integrated atomic moments.

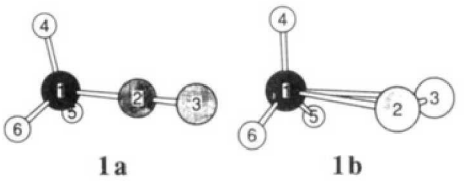

Figure 1. Molecular models of the C_{3v} symmetric minimum **1a** of methyldiazonium ion and its transition-state structure for automerization **1b** as determined at the MP2(full)/6-31G* level.

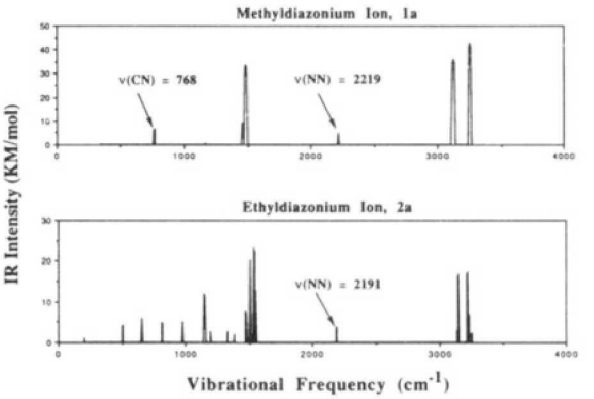

Figure 2. IR spectra of methyldiazonium ion **1a** and ethyldiazonium ion **2a** shown as computed at the MP2(full)/6-31G* level. The CN stretching is heavily coupled with several vibrational modes. For comparison, the vibration of free N_2 occurs at 2180 cm^{-1}.

Results and Discussion

Energies and vibrational zero-point energies (VZPE) determined at RHF/6-31G* and MP2(full)/6-31G* are summarized in Table I. Total energies computed at various correlated levels with the MP2(full)/6-31G* geometries are documented in Table II, and relative energies obtained at all of these levels are summarized in Table III together with the thermochemical data. The stability of methyldiazonium ion **1** has also been studied with three augmented valence-triple-zeta basis sets, and the total energies and the binding energies determined at those levels are included in Table II. Structural parameters are listed in Tables IV, VI, and VII for the molecules **1**, **2**, and **3**, respectively, and the vibrational frequencies and IR intensities determined at the RHF/6-31G* and the MP2(full)/6-31G* levels for all of these molecules are available as supplementary material.

Methyldiazonium Ion. The methyl cation affinity of nitrogen has been determined experimentally, and its value is crucial for the judgment of the quality of our theoretical work. Foster and Beauchamp first measured the heat of formation of **1**, $\Delta H_f(\mathbf{1})$ = 223 kcal/mol, by ion cyclotron resonance spectroscopy.[24] Sub-

(14) Spectrum: Hall, M. K., Department of Chemistry, University of Missouri—Columbia, 1990.

(15) (a) Møller, C.; Plesset, M. S. *Phys. Rev.* **1934**, *46*, 1243. (b) Binkley, J. S.; Pople, J. A. *Int. J. Quantum Chem.* **1975**, *9*, 229. (c) Pople, J. A.; Seeger, R. *Int. J. Quantum Chem.* **1976**, *10*, 1. (d) Pople, J. A.; Krishnan, R.; Schlegel, H. B.; Binkley, J. S. *Int. J. Quantum Chem.* **1978**, *14*, 91.

(16) (a) Hehre, W. J.; Ditchfield, R.; Pople, J. A. *J. Chem. Phys.* **1972**, *56*, 2257. (b) Hariharan, P. C.; Pople, J. A. *Theor. Chim. Acta* **1973**, *28*, 213. (c) Binkley, J. S.; Gordon, M. S.; DeFress, D. J.; Pople, J. A. *J. Chem. Phys.* **1982**, *77*, 3654. (d) Six Cartesian second-order Gaussians were used for d shells.

(17) (a) Krishnan, R.; Binkley, J. S.; Seeger, R.; Pople, J. A. *J. Chem. Phys.* **1980**, *72*, 650. (b) Five pure d orbitals were used and seven pure *f* functions were used in conjunction with the valence-triple-zeta basis sets. (c) Diffuse functions: Clark, T.; Chandrasehkar, J.; Spitznagel, G. W.; Schleyer, P. v. R. *J. Comput. Chem.* **1983**, *4*, 294.

(18) For reviews and comprehensive lists of references, see, for example: (a) Bader, R. F. W. *Acc. Chem. Res.* **1985**, *18*, 9. (b) Bader, R. F. W.; Nguyen-Dang, T. T.; Tal, Y. *Rep. Prog. Phys.* **1981**, *44*, 893. (c) Glaser, R. *J. Comput. Chem.* **1989**, *10*, 118.

(19) (a) Handy, N. C.; Schaefer III, H. F. *J. Chem. Phys.* **1984**, *81*, 5031. (b) See ref 11.

(20) Psichk: Lepage, T. J., Department of Chemistry, Yale University, 1988.

(21) Extreme and Proaim: (a) Biegler-Koenig, F. W.; Bader, R. F. W.; Tang, T. H. *J. Comput. Chem.* **1982**, *3*, 317. (b) These programs were ported both to the IBM 4381 by G. Choy and to the Silicon Graphics Personal Iris by R. Glaser.

(22) Programs Netz and Dipoles written by: Glaser, R., Department of Chemistry, University of Missouri—Columbia, 1990.

(23) Program ESI written by: Glaser, R., and Hall, M. K., Department of Chemistry, University of Missouri—Columbia, 1990.

(24) Foster, M. S.; Beauchamp, J. L. *J. Am. Chem. Soc.* **1972**, *94*, 2425.

Table II. Total Energies Calculated with the MP2(full)/6-31G* Geometries[a-e]

	RHF	MP2	MP3	MP4 DQ	MP4 SDQ	MP4 SDTQ
			6-31G* Basis Set			
1a	148.205 333	148.654 704	148.654 860	148.663 569	148.670 064	148.690 868
1b	148.165 202	148.590 051	148.595 564	148.603 826	148.609 542	148.628 773
2a	187.252 777	187.832 530	187.841 558	187.851 525	187.859 087	187.884 362
2c	187.244 253	187.808 858	187.823 153	187.831 800	187.839 110	187.862 569
Me^+	39.230 411	39.325 375	39.341 913	39.344 689	39.345 054	39.346 177
3c	78.309 497	78.552 308	78.576 380	78.578 934	78.581 200	78.588 405
3d	78.308 977	78.542 186	78.567 746	78.570 782	78.573 397	78.579 615
N_2	108.935 403	109.255 276	109.246 063	109.252 062	109.257 076	109.272 989
			6-311G** Basis Set			
1a	148.243 199	148.728 552	148.727 274	148.736 005	148.743 608	148.769 013
1b	148.202 257	148.662 319	148.666 243	148.674 951	148.681 901	148.705 328
2a	187.299 622	187.934 638	187.943 458	187.953 030	187.961 674	187.992 794
2c	187.294 516	187.911 820	187.925 322	187.933 812	187.942 191	187.971 118
Me^+	39.243 570	39.356 178	39.374 916	39.377 772	39.378 110	39.379 698
3c	78.334 441	78.613 366	78.640 390	78.642 235	78.644 267	78.653 397
3d	78.331 454	78.600 666	78.629 219	78.631 537	78.633 967	78.642 087
N_2	108.960 816	109.296 782	109.283 791	109.290 449	109.296 790	109.316 157
			6-311++G** Basis Set			
1a	148.244 542	148.731 181	148.729 936	148.738 632	148.746 265	148.771 861
Me^+	39.243 728	39.356 520	39.375 267	39.378 122	39.378 453	39.380 056
N_2	108.963 105	109.301 350	109.287 636	109.294 554	109.301 078	109.320 914
E_b		46.00	42.06	41.39	41.88	44.48
			6-311G(df,p) Basis Set			
1a	148.247 610	148.772 103	148.772 416	148.779 358	148.786 846	148.814 884
Me^+	39.243 840	39.365 593	39.384 961	39.387 711	39.388 027	39.389 894
N_2	108.962 631	109.326 893	109.315 094	109.320 345	109.326 587	109.347 834
E_b		49.96	45.41	44.74	45.33	48.42
			6-311++G(df,p) Basis Set			
1a	148.249 259	148.774 632	148.774 924	148.781 843	148.789 345	148.817 560
Me^+	39.244 032	39.365 919	39.385 284	39.388 032	39.388 350	39.390 222
N_2	108.965 131	109.331 458	109.318 847	109.324 359	109.330 751	109.352 470
E_b		48.48	44.42	43.58	44.04	46.98

[a] Total energies ($-E$) in atomic units. All MP_x energies are calculated by using the frozen core approximation. [b] The basis set 6-31G* uses six Cartesian *d* functions, and five pure *d* functions were used with the 6-311G** basis set. Sets of seven pure *f* functions were used in the 6-311G(df,p) basis sets. [c] **3c** calculated in C_s symmetry. [d] Binding energies E_b of **1a** are given in kilocalories per mole; see Table III for further reaction energies. [e] For binding energies of **1a**, see also: Ikuta, S. *J. Chem. Phys.* **1989**, *91*, 1376.

Table III. Relative Energies and Thermodynamic Functions

	RHF/6-31G*		MP2(full)/6-31G*					MPx(fc)6-31G*// MP2(full)/6-31G*					MPx(fc)/6-311G**// MP2(full)/6-31G*				
								MP4					MP4				
reaction	ΔE	ΔVZPE[a]	ΔE	ΔVZPE[a]	$\Delta\Delta H$	$\Delta\Delta S$	$\Delta\Delta G$	MP2	MP3	DQ	SDQ	SDTQ	MP2	MP3	DQ	SDQ	SDTQ
1a → $Me^+ + N_2$	26.02	−5.05	47.13	−5.21	−3.68	31.83	−13.16	46.47	41.97	41.93	42.63	44.99	46.38	43.03	42.53	43.11	45.91
1a → **1b**	24.21	−3.87	41.08	−3.14	−3.19	3.83	−4.33	40.57	37.21	37.49	37.98	38.96	41.56	38.30	38.31	38.72	39.96
2a → **3c** + N_2	5.79[b]	−4.79[b]	16.12	−4.65	−3.05	31.44	−12.41	15.65	11.99	12.88	13.06	14.41	15.37	12.10	12.77	12.94	14.58
2a → **2b**	3.52	−0.12															
2a → **2c**	5.41	−4.38	15.29	−4.32	−3.28	9.51	−6.12	14.85	11.55	12.38	12.54	13.68	14.32	11.38	12.06	12.23	13.60
2a → **2d**	5.47	−4.44															
3a → **3b**	1.19	−0.28															
3c → **3b**	0.38	−0.60															
3a → **3c**	0.81	0.32															
3a → **3d**	0.64	−0.16															
3c → **3d**			6.40	−1.01	−1.03	1.50	−1.48	6.35	5.42	5.12	4.90	5.52	7.97	7.01	6.71	6.46	7.10

[a] ΔVZPE = $\sum$VZPE(products) − $\sum$VZPE(reagents) in kilocalories per mole. RHF/6-31G* values are scaled (factor 0.9); MP2(full)/6-31G* values are unscaled. ΔH and ΔG in kilocalories per mole; ΔS in calories per mole per degree Kelvin. [b] Relative energies for the reaction **2a** → **3a** + N_2.

sequently, these workers and Williamson measured the photoionization appearance potential of **1** from $CH_3N_2CH_3$ and obtained ΔH_f(**1**) = 209.4 kcal/mol.[25] The combination with the latest value for the heat of formation of $CH_3N_2CH_3$,[26] ΔH_f-($CH_3N_2CH_3$) = 35.5 kcal/mol, gave ΔH_f(**1**) = 212.9 kcal/mol.[27] With $\Delta H_f(CH_3^+)$ = 261.2 kcal/mol,[28] these three ΔH_f(**1**) values yield methyl cation affinities for N_2 of 38.2,[24] 51.2,[25] and 48.3[27] kcal/mol, respectively.

(a) Electron Correlation Effects on Structures. In Figure 1 the MP2(full)/6-31G* optimized geometries of the C_{3v} symmetric minimum **1a** and of the C_s symmetric edge-on transition-state structure for automerization **1b** (i214.6 cm^{-1}, a″) are shown. In Figure 2 the IR spectrum of **1a** is shown as computed at the MP2(full)/6-31G* level. Additionally, the effect of electron correlation on the structure of **1a** was determined at the level

(25) Foster, M. S.; Williamson, A. D.; Beauchamp, J. L. *Int. J. Mass Spectrom. Ion Phys.* **1974**, *15*, 429.
(26) Rossini, F. D.; Montgomery, R. L. *J. Chem. Thermodyn.* **1978**, *10*, 465.
(27) McMahon, T. B.; Heinis, T.; Nicol, G.; Hovey, J. K.; Kebarle, P. *J. Am. Chem. Soc.* **1988**, *110*, 7591.
(28) Traeger, J. C.; McMoughlin, R. G. *J. Am. Chem. Soc.* **1981**, *103*, 3607.

Table IV. Structures of Methyldiazonium Ion (**1**)[a-c]

	1a			1b	
parameter	HF	MP2	MP2-VTZ	HF	MP2
C-M	1.5100	1.4602	1.4596	2.6891	2.2858
N2-N3	1.0730	1.1276	1.1185	1.0810	1.1371
	(1.0780)	(1.1300)	(1.1190)		
C-H4	1.0780	1.0915	1.0910	1.0772	1.0865
C-H5	(1.0784)	(1.0887)	(1.0908)	1.0774	1.0871
H4-C-M	105.00	106.10	105.96	90.87	92.81
H5-C-M				90.75	93.00
H4-C-H5				119.96	119.78

[a] Structures optimal at HF/6-31G* (HF), MP2(full)/6-31G* (MP2), and MP2(full)/6-311G** (MP2-VTZ) in angstroms and degrees. [b] M is N_2 for **1a**, and M is the midpoint of N_2 in **1b**. [c] Values in parentheses are those of free N_2 and methyl cation. [d] Energies at MP2(full)/6-311G**: −148.784934 (**1a**), −39.374322 (Me^+), and −109.334062 (N_2), E_b = 48.08 kcal/mol.

Table V. Basis Set Dependencies of the RHF and MP4(SDTQ) Total Energies[a,b]

	RHF/6-31G*				MP4(SDTQ)			
	B	C	D	E	B	C	D	E
				Methyldiazonium Cation, **1a**				
A	23.76	24.60	26.53	27.56	49.04	50.82	77.82	79.56
B		0.84	2.77	3.80		1.79	28.78	30.46
C			1.93	2.96			27.00	28.68
D				1.03				1.68
				Methyl Cation, CH_3^+				
A	8.26	8.36	8.43	8.55	21.03	21.26	27.43	27.64
B		0.10	0.17	0.29		0.22	6.40	6.60
C			0.07	0.19			6.17	6.38
D				0.12				0.21
				Molecular Nitrogen, N_2				
A	15.95	17.38	17.09	18.65	22.09	30.07	46.97	49.87
B		1.44	1.14	2.71		2.99	19.88	22.79
C			−0.30	1.27			16.89	19.80
D				1.57				2.91

[a] Each element specifies the reduction of the total energy (in kilocalories per mole) calculated with the basis set listed on top with regard to the energy calculated with the basis set listed on the left. Basis sets are abbreviated as follows: A = 6-31G(d); B = 6-311G(d,p); C = 6-311++G(d,p); D = 6-311G(df,p); E = 6-311++G(df,p). [b] All values are based on the MP2(full)/6-31G(d) geometries.

MP2(full)/6-311G**. Results are summarized in Table IV. Structural optimizations of **1a** at MP2(full)/6-31G* shorten the CN bond by 0.050 Å and lengthen the NN bond by 0.055 Å, compared to the RHF/6-31G* data. The structure of **1a** determined at MP2(full)/6-311G** is only slightly different. Optimization of **1b** greatly reduces the CN distances, but the diazo group remains essentially disconnected in the transition-state structure for automerization.

(b) Binding Energies. While the RHF binding energies all are too low,[29] we had found previously that the inclusion of perturbational corrections for electron correlation significantly increases the binding energies. For example, a binding energy of 37.3 kcal/mol is found at the level MP4[SDQ]/6-31G*//RHF/6-31G* + VZPEs.[9] With optimal correlated level structures, the dediazoniation of **1a** is found to be endothermic by 47.13 (MP2(full)/6-31G*) and 48.08 kcal/mol (MP2(full)/6-311G**), respectively.

We have computed the binding energies of **1a** at several levels of Møller–Plesset perturbation theory with the MP2(full)/6-31G* structures of **1a** and its fragments. These computations were carried out with the 6-31G* and 6-311G** basis sets, as well as with larger basis sets 6-311++G**, 6-311G(df,p), and 6-311++G(df,p). The latter basis sets result from the augmentation of the 6-311G** basis set with sets of diffuse sp shells on all heavy atoms and diffuse *s* functions on the hydrogens, 6-311++G**, or from the addition of the second-order polarization functions (*f*-type functions) to all heavy centers, 6-311G(df,p), or from both, 6-31++G(df,p). From results summarized in Tables II and III, some trends are apparent. It is found that the MP3-derived binding energies generally are smaller than the MP2-derived values. The fourth-order treatment increases the binding energy again, and values result that are between the MP2- and the MP3-binding energies and closer to the MP2-binding energies. The binding energies calculated at the MP4[SDTQ] level range from 44.48 (6-311++G**) to 48.42 kcal/mol (6-311G(df,p)), and our best estimate for the binding energy is 46.98 kcal/mol (6-311++G(df,p)). Although our best theoretical model, MP4(SDTQ=fc)/6-311++G(df,p)//MP2(full)/6-311G**, certainly deserves the attribute "higher level", the analysis of the basis set effects on the total energies suggests that the binding energy obtained at this higher level might still be a few kilocalories per mole in error. Table V lists the decreases in the total energies of **1a**, CH_3^+, and N_2 that result from improving the 6-31G* basis set. Each element specifies the reduction of the total energy (in kilocalories per mole) calculated with the basis set listed on top with regard to the energy calculated with the basis set listed on the left. The four columns on the left or right show the energy lowering at the RHF or the MP4[SDTQ=fc] levels, respectively. Replacement of the 6-31G* basis set with the 6-311G** basis set causes the expected large decrease in the RHF energies for all of the molecules. Further basis set augmentation has but a marginal effect on the energy of methyl cation; the additional diffuse and second-order polarization functions reduce the energy by only 0.29 kcal/mol. The 6-311G** energies of **1a** and N_2 are comparatively close to the Hartree–Fock limit, although additional functions still lower the energies by a couple of kilocalories per mole. The second-order polarization functions are most beneficial for the description of **1a**, whereas N_2 benefits more from the diffuse functions. The latter probably reflects the ability of diffuse functions to improve the description of lone pairs. *The basis set effects on the correlated energies are of a significantly different quality and quantity.* While the diffuse functions do lower the total energies by a couple of kilocalories per mole, the supplementation of the valence-triple-zeta basis sets with *f* functions causes large decreases of the total energies for all of the molecules. That is, basis sets that are more complete than the 6-311++G(df,p) basis sets are likely to further decrease the total energies, and consequently, the binding energy might be affected.

(c) Thermochemistry. To compare the computed and the experimental binding energies, the calculated values still have to be converted to enthalpies. With the geometries and vibrational frequencies determined at the MP2(full)/6-31G* level, the molecular partition functions have been computed and the thermodynamic functions enthalpy, entropy, and free enthalpy (ΔH, ΔS, and ΔG, respectively) have been determined for standard conditions (Table I). With Table III, the effects of the thermodynamic functions on various reactions can be seen. For example, $\Delta\Delta H$ signifies the difference between the ΔH values of the products and the reagents, and the reaction enthalpy is then determined as the sum of $\Delta\Delta H$ and ΔE, where ΔE is the difference between the total energies of the products and the reagents in the vibrationless state at absolute zero.

The correction for the vibrational zero-point energies (determined at MP2(full)/6-31G*) reduces the ΔE values of 47.13 (MP2(full)/6-31G*), 48.08 (MP2(full)/6-311G**), 45.91 (MP4[SDTQ]/6-311G**//MP2(full)/6-31G*), and 46.98 kcal/mol (MP4[SDTQ]/6-311++G(df,p)//MP2(full)/6-311G**) by 5.21 kcal/mol to 41.92, 42.87, 40.70, and 41.77 kcal/mol, respectively, while the consideration of the enthalpy changes (also computed at MP2(full)/6-31G*) reduces the reaction energies by 3.68 kcal/mol to 43.45, 44.40, 42.23, and 43.30 kcal/mol, respectively.

The consideration of the enthalpy changes instead of the vibrational zero-point energies alone does increase the reaction energies by 1.5 kcal/mol, but nevertheless, they remain about 5

(29) For example, binding energies of 28.5 (4-31G: Vincent, R.; Radom, L. *J. Am. Chem. Soc.* **1978**, *100*, 4306), 25.5 (DZ+P: Demontis, P.; Ercoli, R.; Gamba, A.; Suffritti, G. B.; Simonetta, M. *J. Chem. Soc., Perkin Trans. 2* **1981**, 488), 26.0 (6-31G*: Ford, G. P. *J. Am. Chem. Soc.* **1986**, *108*, 5104), and 21.0 (6-31G* + VZPEs: ref 9) were reported at the RHF level.

Table VI. Structures of Ethyldiazonium Ion (**2**)[a]

parameter	2a HF	2a MP2	2b HF	2c HF	2c MP2	2d HF
N8–N9	1.0733	1.1288	1.0732	1.0793	1.1307	1.0793
C1–N8	1.5732	1.4850	1.5608	3.2070	3.1828	3.2489
C1–C2	1.5151	1.5201	1.5335	1.4325	1.3805	1.4323
C1–H3	1.0783	1.0935	1.0782	1.0783	1.0878	1.0783
C1–H5					1.3132	
C2–H5	1.0846	1.0929	1.0813	1.1154	1.2967	1.1157
C2–H6	1.0811	1.0902	1.0803	1.0811	1.0877	1.0810
C1–N8–N9	179.23[b]	178.08[b]	179.93[b]			80.44
C2–C1–N8	108.42	109.38	109.45	108.15[c]	108.43[c]	117.08
H3–C1–C2	115.72	114.53	115.89	121.37	120.63	121.41
H3–C1–H4	111.92	110.34	111.07	117.02	118.73	116.94
H5–C1–C2						
H5–C2–C1	105.89	106.11	112.34	97.81	58.64	97.64
H6–C2–C1	111.79	111.64	109.35	114.79	120.63	114.84
H6–C2–H7	110.44	110.45	109.35	114.65	118.71	114.60

[a] Structures optimized at HF/6-31G* (HF) and MP2(full)/6-31G* (MP2) in angstroms and degrees. See figures for definition of atoms. [b] Atom N9 cisoid with C2. [c] The angle between the vectors C1C2 and C1M is given (M is the midpoint of N_2).

Table VII. Structures of Ethyl Cation (**3**)[a]

parameter	3a HF	3b HF	3c HF	3c MP2[b]	3d HF	3d MP2
C1–C2	1.4310	1.3853	1.3719	1.3806	1.4409	1.4142
C1–H3	1.0786	1.0775	1.0767	1.0877	1.0789	1.0912
C1–H5	1.9286	1.5359	1.3071	1.3058		
C2–H5	1.1162	1.1899			1.0778	1.0855
C2–H6	1.0812	1.0773			1.0968	1.1136
H3–C1–C2	121.41	120.78	120.68	120.68	122.88	123.02
H3–C1–H4	116.98	118.02	118.61	118.64	116.77	116.62
H5–C2–C1	97.66	72.78	58.35	58.03	114.95	116.87
H6–C2–C1	114.85	119.72			107.36	107.05
H6–C2–H7	114.73	117.96			116.77	98.18

[a] Structures optimized at HF/6-31G* (HF) and MP2(full)/6-31G* (MP2) in angstroms and degrees. See figures for definition of atoms. [b] De facto C_{2v} symmetry. Optimized in C_s symmetry starting from the HF structure of **3a**.

kcal/mol lower than the latest experimental value of 48.3 kcal/mol[27] and they are about 5 kcal/mol higher than Foster's earlier value of 38.2 kcal/mol. Since photoionization appearance potentials do not always provide reliable heats of formations for ionic species and because of our theoretical results, it seems likely that the latest experimental value might be a few kilocalories per mole too high. Finally, we note that the difference in the reaction energies computed at the levels MP4[SDTQ]/6-311G** and MP4[SDTQ]/6-311++G(df,p) with the MP2/6-31G* structures is merely 1.07 kcal/mol. We therefore believe that the former level should produce reasonable results for the larger system ethyldiazonium ion **2** (vide infra).

For the N_2-scrambling reaction of **1** via **1b** $\Delta\Delta H$ and ΔVZPE are virtually identical. With the ΔE value of 39.96 kcal/mol determined at MP4(SDTQ)/6-311G**//MP2(full)/6-31G*, our best estimate of the activation barrier for this process is 36.77 kcal/mol. That is, the automerization of **1** involves almost complete disconnection of the diazo group, essentially free N_2 rotation, and reconnection.

Ethyldiazonium Ion. (a) RHF-Potential Energy Surface of Ethyldiazonium Ion. We have examined the potential energy surface (Figure 3 and Table VI) of ethyldiazonium ion (**2**) to determine the most stable structure and to analyze the pathways for rotation about the CC bond and automerization via N scrambling at the RHF/6-31G* level. The structure **2a** with its staggered CC conformation is found to be most stable. In **2b**, the in-plane CH_3 hydrogen eclipses the CN bond and the analytical computation of the Hessian matrix identifies this structure as the transition-state structure (i261.4 cm^{-1}, a″) for the interconversion of the conformers of **2a**. The activation barrier for the methyl rotation is probably well reproduced at this level, and a value of 3.40 kcal/mol is found when vibrational zero-point energy corrections are included. The automerization of **2a** via rotation of the N_2 group could a priori involve either an out-of-plane N_2 rotation via structure **2c** or an in-plane movement via a structure of the type **2d**. Both of these structures have been optimized, and

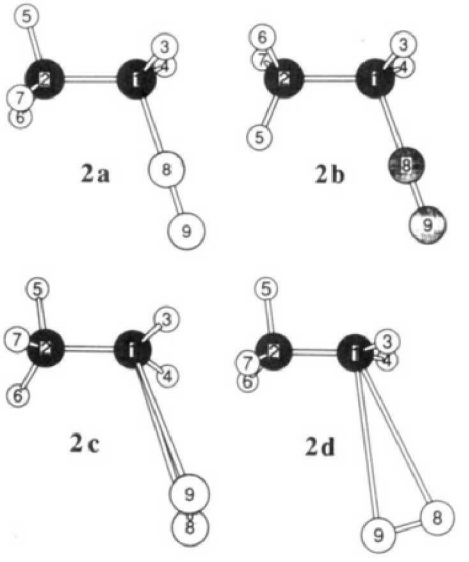

Figure 3. Molecular models of stationary structures on the RHF/6-31G* potential energy surface of ethyldiazonium ion (**2**). **2a** is the single minimum, **2b** is the transition-state structure for rotation around the CC bond, and **2c** is the transition-state structure for automerization.

2c is found to be a transition-state structure (i100.6 cm^{-1}, a″), whereas **2d** corresponds to a second-order saddle point (i101.0 cm^{-1}, a′, i18.2 cm^{-1}, a″) on the potential energy surface. In both of these structures, the CN distances are in excess of 3.2 Å and with C1 carbons nearly sp^2 hybridized. A strong tendency toward formation of an H-bridged structure can be seen in **2c** as well as **2d**—for example, the C1–C2–H5 angle in **2c** is only 97.8°—but the classical topology still persists.

(b) Correlation Effects on the Structures of Ethyldiazonium Ion. **2a** and **2c** have also been optimized at the MP2(full)/6-31G* level

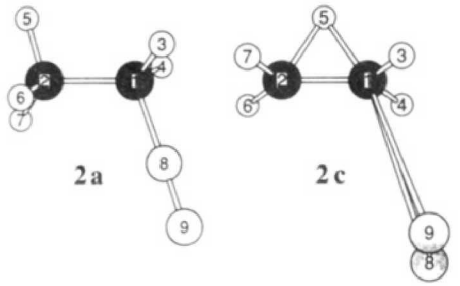

Figure 4. Molecular models of the minimum **2a** and the transition-state structure for automerization **2c** of ethyldiazonium ion as determined at the MP2(full)/6-31G* level.

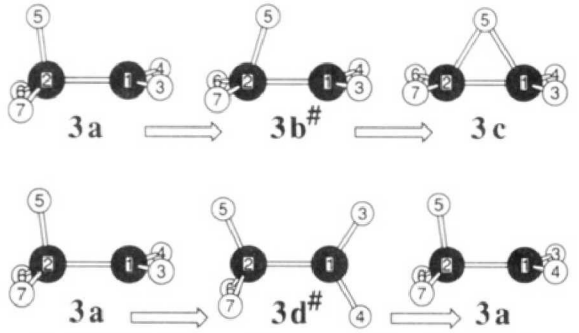

Figure 5. RHF/6-31G* potential energy surface of ethyl cation: Stationary structures along the isomerization pathway between the global minimum **3a** and the local minimum **3c** via the transition-state structure **3b** are shown on top. CC rotation in **3a** is accomplished via the transition state structure **3d** as shown at the bottom.

(Figure 4). While the topology of **2a** persists at this correlated level, the topology of the transition-state structure for the N-exchange process changes drastically. The automerization pathway still involves the out-of-plane rotation of the N_2 group (imaginary frequency of i85.6 cm^{-1}, a″), but the essentially complete disconnection of this group results in the bridging of the in-plane transoid hydrogen. As to the minimum **2a**, we note that there is only a small increase in the CN bond length (0.025 Å) as compared to **1a** and that the NN bond lengths in **1a** and **2a** are virtually alike. The calculated IR spectrum of **2a** (Figure 2) shows that the frequency of the NN stretching vibration is smaller than the one for **1a**: Compared to free N_2 (2180 cm^{-1}) the NN stretching frequency is increased by 29 cm^{-1} for **1a** but only by 11 cm^{-1} for **2a**.

(c) RHF-Potential Energy Surface of Ethyl Cation. On the RHF/6-31G* potential energy surface[30] (Figure 5 and Table VII), the classical structure **3a** (C_s) is the most stable minimum. In **3a**, the CH_3 hydrogen that is aligned with the normal vector of the CH_2 group, H3, is bent significantly toward the CH_2 group, indicative of hyperconjugation. Further reduction of the H3–C2–C1 angle leads to the transition-state structure **3b**, the saddle point connecting **3a** and the nonclassical, H-bridged, local minimum **3c** (C_{2v}) as indicated by the transition vector (i429.1 cm^{-1}, a′) of **3b**. In contrast to **3a**,**b**, in **3d** one of the CH_3 hydrogens and the CH_2 group are eclipsed. At the RHF/6-31G* level **3d** represents the transition-state structure (i278.7 cm^{-1}, a″) for narcissistic automerization of **3a** via CH_3 rotation (Figure 5, bottom). The mechanism for H scrambling between the two carbon centers thus would seem to involve the narcissistic isomerization **3a** → **3d** → **3a**′ and the H-transfer reaction **3a** → **3b** → **3c** → **3b** → **3a**.[31]

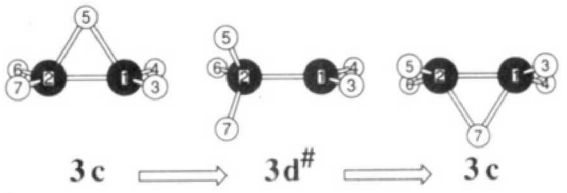

Figure 6. Molecular models of the nonclassical ethyl cation **3c** and of the transition-state structure for H scrambling **3d** as determined at the MP2(full)/6-31G* level.

(d) Correlation Effects on the Potential Energy Surface of Ethyl Cation. The characteristics of the potential energy surface of ethyl cation change dramatically upon inclusion of correlation effects. At the MP2(full)/6-31G* level, the classical structure **3a** is no longer a minimum and the H-bridged cation **3c** becomes the single minimum[32] (Figure 6). A structure that resembles the transition state for CH_3 rotation at the RHF/6-31G* level also is found to be a transition-state structure on the MP2(full)/6-31G* surface. However, on the MP2(full)/6-31G* surface **3d** serves a different purpose: The transition vector (i339.8 cm^{-1}, a″) identifies **3d** as the transition-state structure for the scrambling of the bridging hydrogen atom (Figure 6). Thus, at this level the exchange of hydrogen atoms between the two carbon centers involves a sequence of two exchanges of the bridging H atom. In contrast to the RHF results, there is a clear preference for the H-bridged structure at the correlated levels (Table III). The activation barrier for the process **3c** → **3d** amounts to 6.40 kcal/mol at MP2(full)/6-31G* and to 7.10 kcal/mol at the highest level employed, MP4(SDTQ=fc)/6-311G**//MP2(full)/6-31G*. Inclusion of vibrational zero-point energy corrections of $\Delta VZPE = -1.01$ kcal/mol determined at MP2(full)/6-31G* or the consideration of the $\Delta\Delta H$ value of −1.03 kcal/mol reduces this barrier by about 1 kcal/mol. Thus, the H scrambling in **3** should be a facile process even at low temperature. This finding is in agreement with the experimental observation of the rapid scrambling of deuterium or ^{13}C labels in S_N1 reactions of suitable precursors.[33]

(e) Stability of Ethyldiazonium Ion. At the RHF/6-31G* level the dissociation **2a** → **3c** + N_2 is endothermic by 5.79 kcal/mol and the activation barrier for the N-scrambling process **2a** → **2d** is endothermic by 5.47 kcal/mol. As with **1**, both of these values are severely underestimated. While the complete disconnection of the diazo group leads to the classical ethyl cation **3a** at the RHF level, such disconnection leads to the H-bridged structure **3c** at the correlated level. Just the same behavior is found for the N-scrambling pathway, because the N_2 rotation via **2c** involves virtually complete disconnection of the CN bond. The dediazoniation **2a** → **3c** + N_2 is endothermic by 16.12 kcal/mol at the MP2(full)/6-31G* level and significantly more endothermic compared to the RHF/6-31G* result. The automerization **2a** → **2c** is endothermic 15.29 kcal/mol at MP2(full)/6-31G*. As indicated by the geometry of **2c**, there is barely any interaction between the cation and N_2 in **2c**. As with the methyldiazonium ion, the N_2 scrambling does require essentially complete disconnection. At our highest level, MP4(SDTQ=fc)/6-311G**//

(30) Ethyl cation was previously well studied at many levels of theory. See, for example: (a) Hariharan, P. C.; Lathan, W. A.; Pople, J. A. *Chem. Phys. Lett.* **1972**, *14*, 385. (b) Zurawski, B.; Ahlrichs, R.; Kutzelnigg, W. *Chem. Phys. Lett.* **1973**, *21*, 309. (c) Apeloig, Y.; Schleyer, P. v. R.; Pople, J. A. *J. Am. Chem. Soc.* **1977**, *99*, 5901. (d) Lischka, H.; Koehler, H.-J. *J. Am. Chem. Soc.* **1978**, *100*, 5297. (e) White, J. C.; Cave, R. J.; Davidson, E. R. *J. Am. Chem. Soc.* **1988**, *110*, 6308. (f) Klopper, W.; Kutzelnigg, W. *J. Phys. Chem.* **1990**, *94*, 5625.

(31) The activation barriers for these isomerizations are given in Table III together with the corrections for the vibrational zero-point energies. It is interesting to note that the relative energies when corrected in the usual way for the (scaled vibrational) frequencies would seem to indicate that **3b** and **3c** are both less stable than **3a** by 0.91 (**3b**) and 1.13 (**3c**) kcal/mol, but that **3c** *is in fact more stable than* **3b** *when the VZPEs are taken into account.* However, the RHF/6-31G* surface does not give an adequate representation of ethyl cation (vide infra), and this point therefore needs no further elaboration.

(32) The bridged isomer was found experimentally to be the dominant species in the gas phase by neutralized ion-beam spectroscopy: Gellene, G. I.; Kleinrock, N. S.; Porter, R. F. *J. Chem. Phys.* **1983**, *78*, 1795.

(33) (a) Roberts, J. D.; Yancey, J. A. *J. Am. Chem. Soc.* **1952**, *74*, 5943. (b) Olah, G. A.; DeMember, J. R.; Schlosberg, R. H.; Halpern, Y. *J. Am. Chem. Soc.* **1972**, *94*, 156. (c) Vorachek, J. H.; Meisels, G. G.; Geanangle, R. A.; Emmel, R. H. *J. Am. Chem. Soc.* **1973**, *95*, 4078. (d) Ausloos, P.; Rebbert, R. E.; Sieck, L. W.; Tiernan, T. O. *J. Am. Chem. Soc.* **1972**, *94*, 8939.

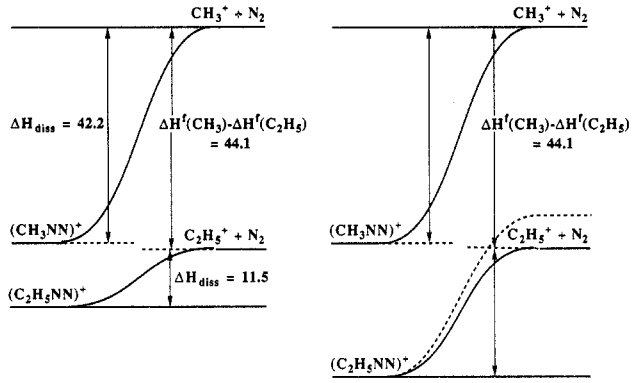

Figure 7. Energy level diagram for the dediazoniation reactions of methyl- and ethyldiazonium ions. The diagram on the left shows the energy levels obtained with the reaction enthalpies computed at the highest common theoretical level. The diagram on the right schematically shows the scenario that might have been anticipated on the basis of the structural and IR spectroscopic differences between **1a** and **2a** as well as on the basis of the changes in their topological properties. See text for discussion.

MP2(full)/6-31G*, slightly smaller ΔE values of 14.58 and 13.60 kcal/mol are obtained for the dediazoniation and the N-scrambling process, respectively. With the consideration of the $\Delta\Delta H$ values of Table III, we obtain our best estimates for the reaction enthalpies: 11.53 kcal/mol for the dediazoniation and 10.32 kcal/mol for the automerization.

Surely one interesting and perhaps even surprising result is the remarkable difference in the thermodynamic stabilities of **1a** and **2a** toward dediazoniation: *The reaction enthalpy for dediazoniation of the methyldiazonium ion is 30.68 larger than that for the ethyldiazonium ion* at the highest common theoretical level, (MP4[SDTQ]/6-311G**//MP2(full)/6-31G* $+\Delta\Delta H$(MP2-(full)/6-31G*). On the left in Figure 7, the energy profiles are shown for the dissociations of the two diazonium ion systems. The energy level for the dissociated methyl ion and N_2 lies 44.1 kcal/mol above the energy level of ethyl cation and free N_2 because of the difference in the experimental heats of formation of the methyl cation (ΔH^f = 261.2) and the ethyl cation[34] (ΔH^f = 217.1 kcal/mol). Clearly, this difference cannot be explained with the structural differences (CN and NN bond lengths) or the differences in the IR frequencies of the NN stretching vibration (vide supra). It is also quite clear from the discussion of the potential energy surface of $C_2H_5^+$ (vide supra) that the formation of the nonclassical ethyl cation can only account for a small part of this enormous stability difference but certainly not for the fact that the dissociation energy of **2** is merely 25% of that found for **1**. If we take (correctly) **3d** as the most stable classical structure of **3**, then we can estimate the reduction in diazonium stability due to the formation of the nonclassical ethyl cation by the relative energy of **3d** with regard to **3c**. This relative energy is ΔE = 7.10 kcal/mol and, when corrected for ΔH, it is 5.62 kcal/mol. Thus, *the intrinsic stabilities of the CN linkages in* **1** *and* **2** *differ by the remarkable amount of 25.1 kcal/mol.* Qualitatively one might argue that the CN linkage in **2** should be somewhat less strong compared to that in **1** simply because (the open form of) ethyl cation would be expected to be a weaker Lewis acid compared to CH_3^+, and a scenario such as depicted on the right in Figure 7 might have been anticipated: The dissociation to the hypothetical classical ethyl cation (dashed path) would require somewhat less energy than the dissociation of **1**, and the extra stabilization of the ethyl cation due to H bridging reduces the dissociation energy a few kilocalories per mole more (solid path). Why is it then that we find this large difference in stability? In search for an answer to this question we have studied the electronic structures of **1** and **2**.

(34) (a) Determined via the ionization potential of the radical by photoelectron spectroscopy: Houle, F. A.; Beauchamp, J. L. *Chem. Phys. Lett.* **1977**, *48*, 457. (b) The CRC handbook lists an older value of $\Delta H^f(C_2H_5^+)$ of 219.0 kcal/mol: *CRC Handbook of Chemistry and Physics*, 66th ed.; Weast, R. C., Ed.; CRC Press: Boca Raton, FL, 1986; p E-80.

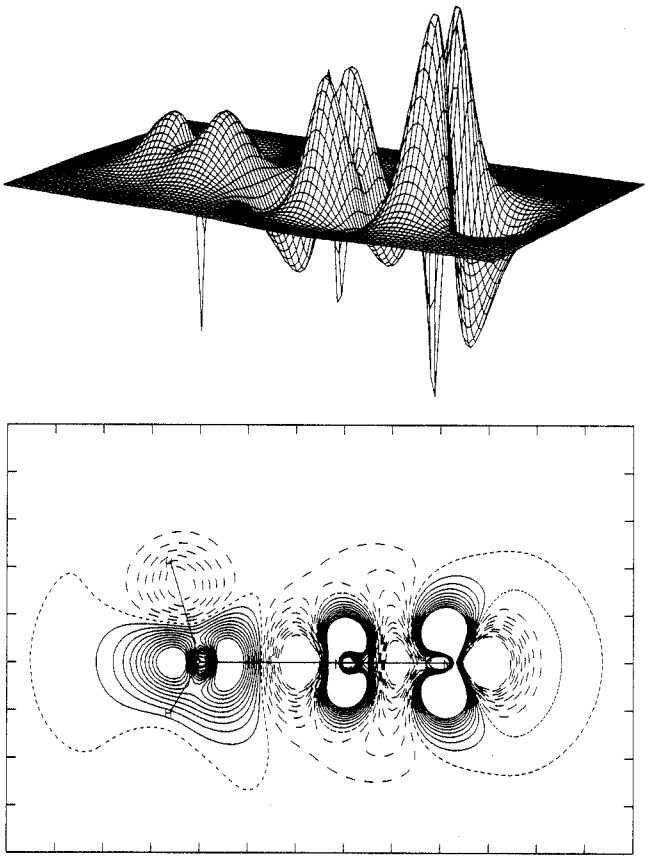

Figure 8. Plots of the electron density difference function $\Delta\rho$ = ρ(MP2(full)/6-31G*) − ρ(RHF/6-31G*) of methyldiazonium ion **1a** for one of the σ_v planes. The surface plot shown on top impressively demonstrates the effects of electron correlation and, in particular, it clearly shows the effects in the core regions. The contour plot shown at the bottom was generated with contour level settings from −0.01 to 0.01 with a spacing of 0.001 (electrons au^{-3}). Positive regions of $\Delta\rho$ are contoured with solid lines, the zero-level contour is short-dashed, and negative regions of $\Delta\rho$ are contoured with long-dashed lines.

Correlation Effects on the Electron Density of Methyldiazonium Ion. In Figure 8, the electron density difference function is shown that results by subtracting the RHF/6-31G* density from the MP2(full)/6-31G* density (both of which were calculated with the MP2(full)/6-31G* optimized structure). Electron correlation causes a reduction of electron density in the NN bonding region, in the lone pair region of the terminal nitrogen, in the CN-bonding region near nitrogen, and in the core regions of all of the heavy atoms. Increases in the electron density function due to correlation are found in the p_x/p_y regions of both of the nitrogens and in the C–p_z region. The effects of electron correlation on the N_2 group might be well described as the result of excitations from the N_σ bonding and nonbonding orbitals into the antibonding N_2 e orbitals and a simultaneous transfer of electron density from the N_2 group into the p_z-type region of the carbon atom. The electron density difference function was also computed in several planes parallel to the one shown in Figure 8, and the plots obtained are fully consistent with this view. To quantify the effects of electron correlation on the three-dimensional electron density function in a convenient way, one can examine the effects on the topological and integrated properties of the molecules.

Several topological parameters can be used to describe this electron reorganization due to correlation. Of special importance is the characterization of the bond critical points, that is, the points in the bonding regions for which the gradient of the electron density vanishes. In Table VIII, the topological parameters are summarized for the MP2 density function as well as for its reference RHF density function. The reported topological values include parameters that describe the locations of the critical points

Table VIII. Topological Properties[a]

bond	r_A	r_B	F	ρ	λ_1	λ_2	λ_3	$\Sigma\lambda_i$	ϵ
				Methyldiazonium Cation					
				MP2(full)/6-31G*//MP2(full)/6-31G*					
C-N	0.458	1.002	0.314	0.204	−0.189	−0.189	0.720	0.343	0.000
N-N	0.604	0.523	0.536	0.592	−1.281	−1.281	0.865	−1.696	0.000
C-H	0.740	0.352	0.678	0.277	−0.805	−0.776	0.509	−1.071	0.038
				RHF/6-31G*//MP2(full)/6-31G*					
C-N	0.443	1.017	0.303	0.194	−0.160	−0.160	1.022	0.702	0.000
N-N	0.606	0.522	0.537	0.607	−1.300	−1.300	0.722	−1.879	0.000
C-H	0.736	0.355	0.675	0.284	−0.829	−0.795	0.489	−1.135	0.042
				Ethyldiazonium Cation					
				MP2(full)/6-31G*//MP2(full)/6-31G*					
C-N	0.469	1.016	0.316	0.193	−0.162	−0.153	0.575	0.261	0.062
N-N	0.602	0.527	0.533	0.592	−1.286	−1.286	0.884	−1.688	0.000
CN-C	0.835	0.685	0.549	0.243	−0.441	−0.440	0.299	−0.582	0.004
CN-H	0.737	0.357	0.674	0.278	−0.803	−0.774	0.513	−1.064	0.037
$C-H_{ip}$	0.719	0.374	0.658	0.270	−0.734	−0.722	0.500	−0.955	0.017
$C-H_{op}$	0.714	0.376	0.655	0.274	−0.745	−0.730	0.504	−0.970	0.021
				RHF/6-31G*//MP2(full)/6-31G*					
C-N	0.450	1.035	0.303	0.181	−0.113	−0.111	0.875	0.652	0.018
N-N	0.603	0.526	0.534	0.607	−1.304	−1.304	0.741	−1.867	0.000
CN-C	0.861	0.660	0.566	0.251	−0.472	−0.470	0.241	−0.702	0.005
CN-H	0.732	0.361	0.670	0.286	−0.827	−0.792	0.492	−1.128	0.043
$C-H_{ip}$	0.710	0.383	0.650	0.276	−0.747	−0.733	0.476	−1.005	0.018
$C-H_{op}$	0.705	0.385	0.647	0.279	−0.757	−0.740	0.478	−1.019	0.023

[a] r_A and r_B are the distances of the critical points from the atoms A and B in angstroms. The parameter F is defined as the ratio $r_A/(r_A + r_B)$. The values of the electron density ρ at the critical points are given in electrons au^{-3}. The λ_i values are the principal curvatures of the electron density at the critical points in electrons au^{-5}, and the Laplacian is their sum. The ellipticity ϵ of the bond is defined as $\epsilon = \lambda_n/\lambda_m - 1$, where $\lambda_n < \lambda_m$ and $\lambda_i < 0$. [b] See supplementary material for topological properties of CH_3^+ for $C_2H_5^+$.

(r_A, r_B, and F), the value of the electron density ρ, the principal curvatures in ρ, and some derived properties as defined in Table VIII. The electron density depletion in the NN-bonding region is reflected in the ρ values of the NN bond critical points of the respective density functions; ρ(RHF) is 0.607, and ρ(MP2) is 0.592. As can be seen, the reduction of electron density in the central NN-bonding region is but marginal. Moreover, the curvature of the electron density perpendicular to the NN axis (λ_1 and λ_2) at the critical point is affected only slightly (λ(RHF) = −1.30 and λ(MP2) = −1.28), indicating a small outward shift of electron density away from the NN axis. Only λ_3, the curvature along the NN bond path, shows a more significant effect; it increases as expected for the correlated density (by about 20%). The parameters that describe the location of the bond critical points (r_A, r_B, and F) remain essentially unchanged for the NN bond critical point. In the RHF density, the CN bond critical point occurs much closer to the carbon than to nitrogen (F = 0.30), and it is characterized by a ρ value of 0.194 and a curvature λ_3 of 1.022. The plots of the density difference function show an electron transfer toward carbon and, as a result, the density is increased to a ρ value of 0.314, the curvature λ_3 is significantly reduced 0.720, and the bond critical point in the MP2 density shifts slightly toward the nitrogen.

Numerical integration of the electron density functions within the atomic basins demarked by the zero-flux surface of the gradient of the density results in the populations shown in Table IX. We note first that the integrated charges obtained at the RHF/6-31G* level with the MP2 optimized structure (CH_3 = +0.86, N_{cent} = −0.38, N_{term} = +0.51) do of course differ slightly from those reported earlier[9] at the RHF/6-31G* level (CH_3 = +0.84, N_{cent} = −0.40, N_{term} = +0.56). Nevertheless, these structure dependencies are small compared to the correlation effects on the population changes. The major effect on the integrated charges is found for the nitrogen atoms: At the correlated level the charge transfer within the N_2 group is reduced. The central and the terminal nitrogens are assigned integrated charges of −0.26 and +0.43, while integrated charges of −0.40 and +0.56, respectively, were found at the RHF level. The carbon shows an increased population at the MP2 level (5.82) compared to the RHF level (5.74), but most of this increase is due to density shifts from the hydrogens (H populations are 0.78 at MP2 and 0.81 at RHF),

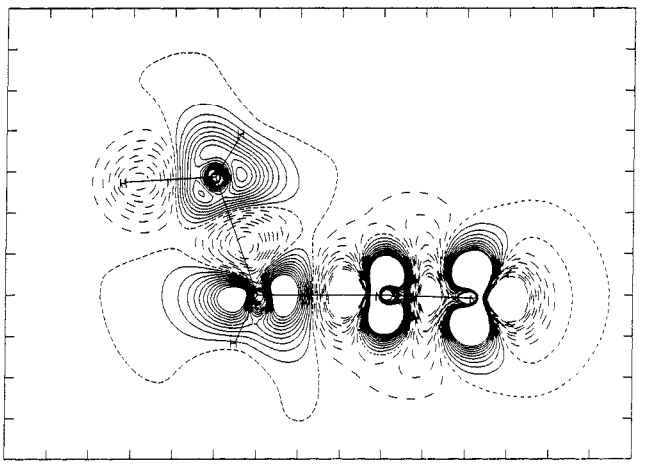

Figure 9. Plot of the electron density difference function $\Delta\rho = \rho$(MP2-(full)/6-31G*) − ρ(RHF/6-31G*) of ethyldiazonium ion **2a** for the C_s plane. The contour level settings are those used for methyldiazonium ion in Figure 8.

and overall the population of the methyl group is but marginally increased at the MP2 level.

Considering these correlation effects on the topological and integrated properties of methyldiazonium ion, we can conclude that *our recently proposed bonding model not only remains valid but emerges even stronger*: CN bonding involves σ donation of electron density from N_2 to the positively charged hydrocarbon fragment and simultaneous π back-donation, and in particular, the electron density accumulation in the CN bonding region occurs *without* major overall charge transfer. The analyses of both the RHF and the correlated electron densities provide compelling evidence that the usual Lewis notations are clearly inadequate since they imply transfer of electron density from N_2 to the hydrocarbon fragment and electron depletion at N_α.

Electronic Structure of Ethyldiazonium Ion. Plots of the electron difference function $\Delta\rho = \rho$(MP2) − ρ(RHF) of **2** have been determined for several planes parallel to the symmetry plane. The plots obtained for the C_s plane are shown in Figure 9, and the following discussion is consistent with the analysis of the function

Table IX. Integrated Properties of Methyl- and Ethyldiazonium Ions[a-c]

atom	IBP	L	T_{int}	T_{corr}
	Methyldiazonium Cation			
	MP2(full)/6-31G*//MP2(full)/6-31G*			
C	5.821	−0.000 11	37.743 71	
N_{cent}	7.256	0.000 19	54.722 32	
N_{term}	6.575	0.000 02	54.065 39	
H	0.783	0.000 05	0.518 51	
total	22.001		148.086 95	
CH_3	8.170		39.299 24	
N_2	13.831		108.787 71	
	RHF/6-31G*//MP2(full)/6-31G*			
C	5.729	−0.002 33	37.576 87	37.772 60
N_{cent}	7.376	0.000 22	54.539 87	54.823 95
N_{term}	6.489	−0.000 23	53.737 60	54.017 50
H	0.803	0.000 06	0.527 56	0.530 31
total	22.003			148.204 96
CH_3	8.138			39.363 53
N_2	13.865			108.841 45
	Ethyldiazonium Cation			
	MP2(full)/6-31G*//MP2(full)/6-31G*			
C(N)	5.819	0.002 70	37.754 71	
C(C)	6.057	−0.000 06	37.918 93	
N_{cent}	7.233	0.000 03	54.709 92	
N_{term}	6.606	−0.000 01	54.088 33	
H at C(N)	0.813	0.000 07	0.536 15	
H_{ip} at C(C)	0.868	0.000 07	0.552 26	
H_{oop} at CC	0.894	0.000 06	0.566 26	
total	29.998		187.228 97	
CH_2	7.445		38.827 01	
CH_3	8.713		39.603 71	
N_2	13.840		108.798 25	
	RHF/6-31G*//MP2(full)/6-31G*			
C(N)	5.787	0.000 18	37.629 49	37.789 68
C(C)	5.912	0.000 27	37.719 80	37.880 37
N_{cent}	7.346	0.000 02	54.520 51	54.752 60
N_{term}	6.526	0.000 02	53.764 06	53.992 93
H at C(N)	0.835	0.000 07	0.547 06	0.549 39
H_{ip} at C(C)	0.903	0.000 07	0.567 95	0.570 37
H_{oop} at CC	0.928	0.000 07	0.581 57	0.584 05
total	30.000			187.252 82
CH_2	7.457			38.888 66
CH_3	8.671			39.618 84
N_2	13.872			108.745 53

[a] Total energies and Virial ratios for the RHF computations: E(**1a**) = −148.205327 hartrees at $-V/T$ = 2.00520861; E(**2a**) = −187.252772 hartrees at $-V/T$ = 2.00425697. The Virial ratio for methyl cation was $-V/T$ = 2.00154321 and for ethyl cation $-V/T$ = 2.00125495. [b] By difference. [c] See supplementary material for integrated properties of methyl and ethyl cations.

$\Delta\rho$ in all other planes as well. The same pattern of electron reorganization is found as in the case of **1**. In addition, it can be seen that the electron density in the CC-bonding region is reduced and that a shift of electron density from all hydrogens to the carbons occurs at the correlated level.

The topological analysis reveals almost identical characteristic values for the NN bond critical point of **2** and **1** (Table VII) at both theoretical levels with only λ_3 being somewhat larger. The examination of the CN regions of **1** and **2** shows that the critical points are virtually at the same location (F values); however, the electron density at those points is 5% smaller for **2** (ρ = 0.19) than for **1** (ρ = 0.20) and the curvatures all are reduced by about 20%. The CC bond in **2** is polarized with the methylene carbon being the more electropositive atom; the CC bond critical point (F = 0.55) is closer to the methylene carbon. With the extrema in the electron density function located, the atomic populations were determined by integration, and the results are summarized in Table IX. As with **1**, the charges obtained from the populations of **2** determined at the RHF (C_2H_5 = +0.87, N_{cent} = −0.35, N_{term} = +0.47) and the MP2 (C_2H_5 = +0.84, N_{cent} = −0.23, N_{term} = +0.39) levels show a smaller amount of internal polarization of the N_2 group, but they are qualitatively similar. We will show

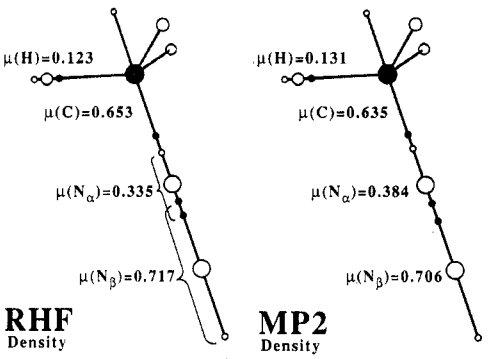

Figure 10. Integrated atomic first moments, calculated with the RHF/6-31G* (left) and with the MP2(full)/6-31G* (right) electron densities based on the MP2 structures, superimposed on the molecular model of the methyldiazonium ion **1a**. The absolute values of the μ vectors are given in atomic units (1 au equals 2.5418 D), and the μ vectors point from the unfilled circles (○) to the filled circles (●).

(vide infra) that this reduced polarization is crucial for an understanding of the difference in the stabilities of **1** and **2**. Comparison of the integrated populations of **1** and **2** (at the MP2 level) reveals further that there are only small differences in the overall charges of the N_2 groups (+0.17 for **1** and +0.13 for **2**) and the hydrocarbon fragments (+0.83 for **1** and +0.84 for **2**). For both of the diazonium ions most of the charge is located on the hydrocarbon fragment and not on the N_2 group, in sharp contrast to the commonly accepted Lewis notation of these species.

The overall charge of the ethyl group in **2** is +0.84, and this charge is distributed over the CH_2 group (+0.56) and the CH_3 group (+0.28) in a ratio of roughly 2:1. The methyl group not only takes over all of the charge of the hydrogen it replaces but also slightly reduces the charges of the methylene hydrogens in **2** (+0.19 compared to +0.22 in **1**) while the integrated populations of the C atom to which the diazo function is attached remain the same (+0.18) in **1** and **2**. Thus, the replacement of one of the methyl hydrogens in **1** by the methyl substituent *essentially moves 0.28 of the positive charge of the hydrocarbon fragment further away from the diazo group.* Certainly, this result might provide (part of) an explanation for the lower stability of **2** compared to **1**. We will address this point further after a discussion of the polarization effects *within* the atomic basins.

Intramolecular Polarization and Electrostatic Interactions. The graphical analysis of the electron density difference functions impressively demonstrates that most of the significant correlation effects manifest themselves within the atomic basins and, in particular, near the core. However, electron density analysis techniques most commonly are used with a focus exclusively on the characterization of the bonding regions. The characterization of extrema of both the one-dimensional type (critical points) and the two-dimensional type (zero-flux surfaces) does not reflect the electron density distribution *within* the basin, and integrated properties account for them to different degrees. Integrated kinetic energies, for example, do account for the electron density distribution within the basin as their evaluation involves gradients of the electron density. However, chemists are more prone to think of electronic structures in terms of charges and to reflect on such charges with the implied assumption that discussions of charge distributions are correlated with energy considerations. Inherently, any information about the electron distribution within the atomic basins is lost in the determination of the integrated populations. To recover the asymmetry of the electron density function within each basin, the discussion of a further and usually neglected integrated property is required or perhaps even mandated: the atomic moment μ. The atomic first moment μ is defined[35] as the negative of the volume integral of $\mathbf{r}'\rho(\mathbf{r})$ taken over the basin, where $\mathbf{r}'$ measures the distance of the position $\mathbf{r}$ from the position of the

(35) (a) Bader, R. F. W.; LaRouche, A.; Gatti, C.; Carroll, M. T.; MacDougall, P. J.; Wiberg, K. B. *J. Chem. Phys.* **1987**, *87*, 1142. (b) Slee, T. *J. Am. Chem. Soc.* **1986**, *108*, 7541.

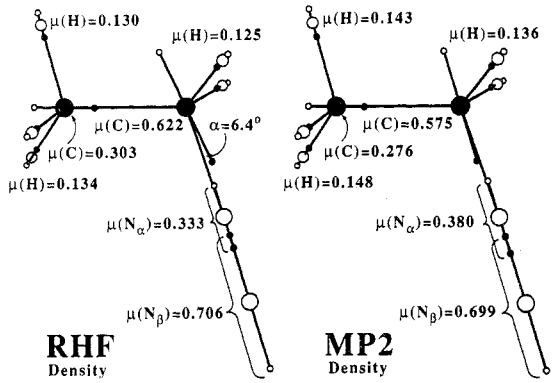

Figure 11. Graphical display of the integrated atomic first moments of ethyldiazonium ion **2a**. See legend to Figure 10.

nucleus Y ($\mathbf{r}' = \mathbf{r} - \mathbf{Y}$). The μ vectors were determined and they are displayed in Figures 10 and 11 for the molecules **1a** and **2a**, respectively. In these figures, the μ vectors (O–●) are superimposed on the molecules and they are directed from the unfilled "O" to the filled "●" markers. The absolute values are given in atomic units, where 1 au equals 2.5418 D. The exact angles enclosed between the directions of the atomic dipole moments and bond directions were determined, and they were found to be negligible in all cases but for the C(N) carbon in **2a** (see Figure 10).

As suggested by the electron density difference functions, we find that electron correlation affects these μ vectors significantly more compared to the bond properties and the integrated populations. Deviations in the order of 5% seem typical, and the differences can become as large as 15%. Furthermore, the absolute values of μ might decrease or increase; that is, electron correlation may act such as to render the electron density within a basin more spherically symmetrical (e.g., C) or it may reinforce its asymmetry to better serve bond formation (e.g., H, N_{cent}). In the following, the μ vectors obtained at the correlated level are discussed unless otherwise noted.

In both **1a** and **2a**, the $\mu(N_{cent})$ vectors are directed toward N_{term} and the $\mu(N_{term})$ vectors are antiparallel and much larger. These directions show that the electron density within the basins of N_{cent} and N_{term}, respectively, are polarized into the CN bonding and the lone pair regions, respectively, and the corresponding $\mu(N)$ values for **1a** and **2a** are virtually alike. The μ vectors of both of the C(N) carbons are directed toward N_{cent}. All of the atoms in the hydrocarbon fragments that are attached via one or two bonds to C(N) show μ vectors that are directed along the respective bonds and toward the electron-deficient center. There is a general relation between the locations of the bond critical points and these atomic moment directions in that the μ vectors are always directed toward the associated bond critical point that is closer.

It is commonly accepted to relate atomic charges to bond stabilities, a practice that has its roots in the domain of ionic compounds. For ion pairs, the binding energies are indeed very well approximated by the Coulombic interaction between the point charges associated with the ions. Accordingly, in polar molecules the bonding between atoms with opposite charges is qualitatively attributed to a covalent and an additional electrostatic component. To test the implied assumption that such electrostatic interactions[36] can be estimated with atom-centered electric moments, we have determined all of the charge/charge, charge/dipole, and dipole/dipole interactions for **1a** and **2a** with the integrated atomic charges and first moments obtained from the MP2(full)/6-31G* electron density. Results are listed in Tables X and XI. Usually the charge/charge interaction is the dominant term for a given

(36) The term "electrostatic interactions" is used here for the electrostatic interactions between the atom-centered point charges and dipoles; it should not be confused with the quantum mechanically defined term that contains all ee, nn, and ne interactions. In our model, all three terms effectively are combined in one term by means of elimination of the nuclear charges via the difference between it and the atom population.

Table X. Intramolecular Electrostatic Interactions of Methyldiazonium Ion **1a**[a,b]

		C1	N2	N3	H4	H5	H6
CC	C1	0.00	−10.45	9.77	11.86	11.86	11.86
CD		0.00	−19.08	10.39	−2.19	−2.19	−2.19
DD		0.00	−7.27	2.40	−0.13	−0.13	−0.13
Σ		0.00	−36.83	22.58	9.54	9.54	9.54
CC	N2		0.00	−32.07	−9.02	−9.02	−9.02
CD			0.00	−2.48	−4.02	−4.02	−4.02
DD			0.00	17.57	−0.11	−0.11	−0.11
Σ			0.00	−16.98	−13.17	−13.17	−13.17
CC	N3			0.00	9.97	9.97	9.97
CD				0.00	3.29	3.29	3.29
DD				0.00	0.07	0.07	0.07
Σ				0.00	13.35	13.35	13.35
CC	H4				0.00	8.64	8.64
CD					0.00	2.51	2.51
DD					0.00	0.09	0.09
Σ					0.00	11.24	11.24
CC	H5					0.00	8.64
CD						0.00	2.51
DD						0.00	0.18
Σ						0.00	11.33
CC	H6						0.00
CD							0.00
DD							0.00
Σ							0.00

[a] All energies are in kilocalories per mole. CC, CD, and DD are the contributions due to charge/charge, charge/dipole, and dipole/dipole interactions between the pairs of atoms, and Σ is the sum of all of these interactions. [b] All values are based on the integrated populations and first atomic moments determined at MP2(full)/6-31G*.

pair, followed by the charge/dipole and dipole/dipole terms in that order. However, since the μ values can become rather large (Figures 8 and 9), there are a few exceptions. For example, in the NN interaction the charge/dipole contributions nearly cancel out, but the dipole/dipole interaction contributes greatly. On the other hand, the attraction between the C(N) carbon and N_{cent} is dominated by the charge/dipole interactions and not by the charge/charge interactions.

The electrostatic contributions, ΔES^{bond}, to the CN bonding are the differences between the overall electrostatic energies of **1a** (+31.74) and **2a** (+27.88), respectively, and the sums of the electrostatic interaction energies of the fragments in the molecules (indicated by the superscript "mol").

$$\Delta ES^{bond}(A\text{–}B) = ES(AB) - [ES(A^{mol}) + ES(B^{mol})] \quad (3)$$

With the values of $ES(CH_3^{mol}) = 62.43$ and $ES(N_2^{mol}) = -16.98$ for **1a** and $ES(C_2H_5^{mol}) = 54.04$ and $ES(N_2^{mol}) = -18.53$ kcal/mol for **2a**, we find the contributions to the CN bonding to be −13.71 kcal/mol for **1a** and −7.63 kcal/mol for **2a**. These values support our conclusion that the CN bonding in the diazonium ions may be attributed in part to the electrostatically favorable quadrupolar charge distribution $R^+N_\alpha^{\delta-}N_\beta^{\delta+}$ in the diazonium ions. Moreover, the difference in the ΔES^{bond} values of **1a** and **2a** reflects that the replacement of one of the methyl hydrogens in **1** by the methyl substituent essentially moves 0.28 of the positive charge of the hydrocarbon fragment further away from the diazo group (vide supra). Note that (a) the consideration of the charge/charge interactions only would indicate *destabilizing* interaction energies of +2.17 (**1a**) and +3.69 kcal/mol, respectively, and that (b) the electrostatic interaction energy calculated either from the charges or from the charges and the dipoles of only the bonded atoms does not even approximate the overall electrostatic interaction energy for that bond. Both of these commonly used approximations should be avoided. While the term $\Delta ES^{bond}(CN)$ accounts for the electrostatic contributions to the CN binding *in* the diazonium ions, further terms need to be considered for the derivation of the CN-binding energies.

Table XI. Intramolecular Electrostatic Interactions of Ethyldiazonium Ion **2a**[a]

		C1	N2	N3	H4	H5	C6	H7	H8	H9
CC	C1	0.00	−9.43	9.04	10.28	10.28	−2.24	3.76	2.93	2.93
CD		0.00	−16.16	9.06	−0.40	−0.40	4.52	−1.46	0.65	0.65
DD		0.00	−3.81	1.27	−0.55	−0.55	−0.93	−0.57	0.13	0.13
Σ		0.00	−29.40	19.38	9.33	9.33	1.35	1.73	3.71	3.71
CC	N2		0.00	−27.01	−7.11	−7.11	1.79	−3.02	−3.00	−3.00
CD			0.00	−1.84	−3.52	−3.52	−1.06	−1.15	−0.92	−0.92
DD			0.00	10.34	−0.06	−0.06	−0.42	−0.09	0.01	0.01
Σ			0.00	−18.53	−10.71	−10.71	0.31	−4.27	−3.91	−3.91
CC	N3			0.00	7.98	7.98	−2.17	3.90	3.93	3.93
CD				0.00	2.85	2.85	0.61	1.25	1.02	1.02
DD				0.00	0.03	0.03	0.29	0.07	0.00	0.00
Σ				0.00	10.87	10.87	−1.27	5.23	4.95	4.95
CC	H4				0.00	6.48	−1.59	3.24	2.12	2.59
CD					0.00	2.26	1.44	0.65	0.68	0.59
DD					0.00	0.20	0.07	0.00	0.02	0.03
Σ					0.00	8.94	−0.09	3.89	2.83	3.21
CC	H5					0.00	−1.59	3.24	2.59	2.12
CD						0.00	1.44	0.65	0.59	0.68
DD						0.00	0.07	0.00	0.03	0.02
Σ						0.00	−0.09	3.89	3.21	2.83
CC	C6						0.00	−2.26	−1.83	−1.83
CD							0.00	−2.74	−2.82	−2.82
DD							0.00	−0.97	−0.36	−0.36
Σ							0.00	−5.98	−5.00	−5.00
CC	H7							0.00	2.61	2.61
CD								0.00	1.58	1.58
DD								0.00	0.05	0.05
Σ								0.00	4.25	4.25
CC	H8								0.00	2.08
CD									0.00	1.41
DD									0.00	0.24
Σ									0.00	3.73
CC	H9									0.00
CD										0.00
DD										0.00
Σ										0.00

[a] See legend of Table X.

To determine the electrostatic contributions to the CN-binding energy, one needs to consider the term ΔES^{bond} together with the changes of the electrostatic energies of the subsystem F (F = A and B) associated with the CN bond formation, ΔES^{frag}

$$\Delta ES^{bind}(A\text{–}B) = \Delta ES^{bond}(A\text{–}B) + \sum ES^{frag}(F) \quad (4)$$

where

$$\Delta ES^{frag}(F) = ES(F^{mol}) - ES(F^{free}) \quad (5)$$

The electrostatic energies of the free isolated subsystems are +92.61 for CH_3^+, +47.90 for $C_2H_5^+$ (**3d**), and +24.18 kcal/mol for N_2 (N in N_2 has an atomic dipole moment of 0.612 au directed toward the bonding region). On formation of **1a**, the methyl fragment is stabilized by −30.18 kcal/mol and N_2 is stabilized by −41.16 kcal/mol, and on formation of **2a** the ethyl cation is *de*stabilized by 6.14 kcal/mol while the N_2 is stabilized by −42.71 kcal/mol. Thus, we obtain for the electrostatic contributions to the CN-binding energies the values of −85.05 kcal/mol for **1a** and −20.02 kcal/mol for **2a**.

A first inspection of these numbers suggests that they are greatly overestimated but that they do show the correct trend. On the basis of this model, one would have to conclude that (a) the large difference in the dissociation energies of **1a** and **2a** is primarily due to the much greater gain in stability of the CH_3 fragment compared to the C_2H_5 fragment and that (b) the stabilities of the N_2 groups in **1a** and **2a** remain essentially the same.

Fragment Energy Analysis and CN Bond Stabilities. The virial theorem ($V = -2T$) holds for the iteratively determined self-consistent Hartree–Fock wave functions,[37] and therefore, the total energy of the molecule can be determined from the kinetic energy alone via the equation $E = -T$. Bader has shown that this theorem also is valid for the atomic basins defined by the zero-flux surface of the electron density, making it possible to determine the energy contributions of atoms and fragments to the overall energy of the molecule.

In a Gedanken experiment the reaction energies for the dissociations of **1a** and **2a** can be decomposed into two components, namely, the energy difference ΔE_1 between the N_2 group in the diazonium ion and free N_2 and the energy difference ΔE_2 between the free cations and the hydrocarbon fragments in the diazonium ions.

		1a	**2a**
$N_2[(RNN)^+] \rightarrow N_2$	ΔE_1	−58.96	−119.15
$R[(RNN)^+] \rightarrow R^+$	ΔE_2	83.39	124.25
$(RNN)^+ \rightarrow R^+ + N_2$	ΔE_{diss}	24.43	5.10

The ΔE_1 values can be determined from the N atom stabilities of **1a** and **2a** together with the total energy of N_2, and they show that the N_2 groups in **1a** and **2a** are *destabilized* and that the N_2

(37) It is not clear at present whether this also holds true for the correlated electron densities. Phenomenologically, it is found that the sum over the integrated atom stabilities greatly differs from the MP2(full)/6-31G* energy and there is no indication that this difference is caused by numerical problems. We therefore discuss the atom stabilities determined at the RHF/6-31G*//MP2(full)/6-31G* level. At this level, the differences between the integrated stabilities and the computed total energies are less than 0.4 kcal/mol after correction of the integrated kinetic energies for the virial defect of the wave function. The total RHF/6-31G*/MP2/6-31G* energies (−*E* in au) are 108.93540 (N_2), 148.20533 (**1a**), 39.23041 (CH_3^+), 187.25278 (**2a**), and 78.30950 (**3c**).

group in **2a** is 60.19 kcal/mol more destabilized than the one in **1a**. The carbocations on the other hand are *stabilized* as the diazonium ions are formed, and in particular, the C_2H_5 fragment is 40.86 kcal/mol more stabilized than the methyl fragment. From these integrated properties, we obtain binding energies of 24.43 and 5.10 for **1a** and **2a**, respectively, which are in close agreement with the directly computed binding energies at that level. While it is commonly assumed that bond formation stabilizes both of the bonded fragments, CN bonding results from stabilization of the hydrocarbon fragment and despite the destabilization of the N_2 group. The cations force N_2 to form diazonium ions.

The charge/dipole and the energy model suggest different reasons for the large difference in the CN bond stabilities in the methyl- and ethyldiazonium ions. The former assigns the large difference to the different degrees of stabilization of the hydrocarbon fragments (with little differences in the N_2 groups), while the latter assigns it to the larger destabilization of the N_2 group in **2a**, which is only in part compensated for by the large stabilization of the ethyl fragment compared to the methyl fragment in the respective diazonium ions. Note especially that the stabilizations of the hydrocarbon fragments are assigned a reversed order in the two models. The most likely reason for this difference is related to the (small) charge transfer from the diazo group to the (heavily charged) hydrocarbon fragment. The small reduction in the overall electron population of the N_2 groups has little effect on the electrostatic model, but it does have a severe effect on the N_2 energy. With the overall charge transfer being essentially the same in both of the diazonium ions, the smaller destabilization of **1a** might be attributed to the gain in energy of the N_2 group as a result of being in the stronger electric field of the more localized charge of the methyl fragment. Similarly, the small increase of the overall population of the hydrocarbon fragment stabilizes both of the hydrocarbon fragments, a feature that is apparently reflected insufficiently in the charge/dipole model.

Conclusion

The dediazoniation of methyldiazonium ion has been examined at the full fourth-order level of Møller–Plesset perturbation theory with geometries optimized at correlated levels (up to MP2(full)/6-311G**) and with valence-triple-zeta basis sets that were augmented both with sets of diffuse and with multiple sets of polarization functions of first and second order (up to 6-311++G(df,p)). At the highest level, we find an enthalpy of 43.3 kcal/mol for the dediazoniation of **1**, a value which is well within the experimental range but that remains a few kilocalories per mole lower than the latest experimental value of 48.3 kcal/mol. The dependency of this reaction enthalpy on the theoretical model suggests that our highest common theoretical level, MP4[SDTQ]/6-311G**//MP2(full)/6-31G*+VZPE(MP2(full)/6-31G*), should result in a reliable value for the difference in the dediazoniation energies of **1** and **2**. At this level, the dediazoniation enthalpies of 42.2 and 11.5 kcal/mol are found for **1** and **2**, respectively.

The *bonding model for aliphatic diazonium ions* previously proposed on the basis of the analysis of the RHF electron density functions *is confirmed at the correlated level.* Electron correlation affects the electron densities of **1** and **2** in a way that can be described as the result of excitations from the N_σ orbitals into the N_2 e* orbitals and a simultaneous transfer of electron density from the N_2 group into the C(N) p_z-type region but with only small consequences for the topological and integrated properties. The charge transfer from N_2 to the hydrocarbon fragment is small. In sharp contrast to the Lewis notations, the aliphatic diazonium ions are best described as carbenium ions, $R^{+(1-\gamma)}N_\alpha^{-\delta}N_\beta^{+(\delta+\gamma)}$, where γ and δ are about 0.2. The charge distribution suggests that CN bonding benefits from the quadrupolar charge distribution indicated. The ΔES^{bond} values were defined to give a more quantitative estimate of this intuitive view, and the calculated ΔES^{bond}(CN) values computed with both the atomic charges *and* the atomic dipoles of *all* atoms do indeed support this notion. The analysis of the fragment stabilities shows that CN bonding in the aliphatic diazonium ions generally is the result of stabilization of the hydrocarbon fragment and N_2 destabilization.

Considering that free ethyl cation is stabilized by 5.6 kcal/mol due to the formation of the nonclassical structure, we obtain the remarkably large value of 25.1 kcal/mol for the intrinsic stability difference of the CN linkages in **1** and **2**. This difference is explained by the charge dispersal in the hydrocarbon fragment of **2** and the larger destabilization of the N_2 group in **2** compared to **1**. We emphasize that the difference in the dediazoniation energies *is not* merely a reflection of features in the CN-bonding regions; in other words, the characterization of the bonding region alone *is not* sufficient to characterize the bond.

The difference in the stabilities of **1** and **2** agrees well with and offers a simple explanation for the experimentally observed difference in their site preferences for alkylation. The lability of **2** causes alkylation exclusively via S_N1-type chemistry, whereas the higher stability of **1** leads to a more selective alkylation at the more nucleophilic sites.

Acknowledgment. This work was supported in part by a National Institutes of Health Institutional Biomedical Research Support Grant (RR 07053). M.K.H. was supported by a Howard Hughes Undergraduate Research Fellowship.

Supplementary Material Available: Tables listing vibrational frequencies and IR intensities of all of the stationary structures of **1–3** determined at the levels RHF/6-31G* and MP2(full)/6-31G*, topological (r_A, r_B, F, ρ, λ_i, ϵ) and integrated (IBP, L, kinetic energy) properties of **1a**, **2a**, **3c**, **3d** and CH_3^+ as determined at the RHF and MP2(full) levels with the 6-31G* basis set and with the MP2(full)/6-31G* geometries, and electrostatic interaction matrices for CH_3^+ and $C_2H_5^+$(**3d**) (12 pages). Ordering information is given on any current masthead page. This material may be obtained directly from the authors via electronic mail (CHEMRG@UMCVMB).